






## Implicit Surface Modelling and Parametric Optimization for Self-cleaning Portable Toilets Using a Rotary Jet Head Cleaning in Grasshopper

Mikhael Johanes<sup>1</sup> , Paramita Atmodiwirjo<sup>2</sup>  and Yandi A. Yatmo<sup>3</sup> 

<sup>1</sup>Universitas Indonesia, [m.johanes@ui.ac.id](mailto:m.johanes@ui.ac.id)

<sup>2</sup>Universitas Indonesia, [paramita@eng.ui.ac.id](mailto:paramita@eng.ui.ac.id)

<sup>3</sup> Universitas Indonesia, [yandiay@eng.ui.ac.id](mailto:yandiay@eng.ui.ac.id)

Corresponding author: Paramita Atmodiwirjo, [paramita@eng.ui.ac.id](mailto:paramita@eng.ui.ac.id)

**Abstract.** This paper describes the development of design and optimization workflow of self-cleaning portable toilet cubicle interior surface in Grasshopper to obtain a high cleaning performance. Modelling of the portable toilet cubicle interior surface was performed using the parametrically defined skeletal implicit modelling technique, which allows for the quick generation of smooth and seamless surface variants. Assuming the importance of impact pressure to cleaning performance, the developed rotary jet head (RJH) cleaning simulation model provides the evaluation and optimization of the cleanability performance of the toilet cubicle interior surface. The distribution of the cleaning effect using a rotating liquid jet for a set of configured surfaces can be described as a function of surface shape and jetting parameters, such as position and motion. The optimization objective is defined as the maximization of cleaning effect distribution and the minimization of under cleaned surfaces. The findings of the study suggest the potential of implicit surface modelling being a promising method within the parametric modelling environment when coupled with a cleaning performance simulation in order to enable the optimization of the surface. In particular, it suggests the appropriate surface configuration for optimum cleaning performance.

**Keywords:** implicit surface, rotary jet head cleaning, model-based optimization, hygienic design, cleaning performance simulation

**DOI:** <https://doi.org/10.14733/cadaps.2020.674-689>

### 1 INTRODUCTION

Cleanability is an aspect of architectural performance that receives little attention yet holds importance to maintain the sustainability of an environment and the wellbeing of the users. The cleanability is particularly critical in hygiene facilities, such as the toilet and bathroom, which are subjected to intensive cleaning labor to maintain usability [22]. Despite its importance in building

maintenance, cleaning is rarely considered during design and construction stages, which leads to expensive maintenance and quick deterioration of building materials [7]. The development of performative-based design via the digital environment is potential to address this issue by understanding the key relationship between cleaning performance and its spatial aspects.

Drawing on the concept of in-place cleaning for industrial application [25], we established the idea of a self-cleaning toilet cubicle cleaned by the available rotary jet head (RJH) cleaning technique. The development of parametric modelling technique and the optimization in digital design provide an arena for experimentation in performative-based design [24]. Optimal design can be achieved by iteratively evaluating the generated design and adjusting the defining parameters [12]. Parameterization of surface modelling and the simulation of cleaning performance allows for the optimization of the architectural surface to comply with cleanability requirements. In this case, the possibility of such optimization has been outlined in the previous study [18]. The study implements an implicit surface modelling technique to quickly produce objects with smooth surfaces that are relevant to hygiene-oriented design in which smoothness and accessibility facilitate cleaning [16]. The ability to easily deform objects using implicit surface modelling technique also allows an easy adjustment in the parametric optimization process. This study describes the optimization of cleanability of a toilet surface through the development of a parametric skeletal implicit surface cubicle model coupled with the development of a simulation of RJH cleaning.

## 2 BACKGROUND: PARAMETRIC MODELLING AND OPTIMISATION OF CLEANING PERFORMANCE

The integration of parametric modelling and numerical simulations enables a finding of an optimal solution within a set of design alternatives [31]. The study presented in this paper intends to develop a parametric design process of architectural surface that is subjected to RJH cleaning. This paper describes the parametric approach that enables the modelling of a surface shape of the toilet cubicle and the simulation of RJH cleaning that takes account the effect of mechanical force of liquid jet impingement on cleaning performance.

### 2.1 Skeletal Implicit Surface Modelling

A smooth and seamless surface configuration is preferred in a hygiene-oriented environment, such as the toilets [22]. The surface needs to be smooth and free of imperfect features to prevent the harbouring of microorganism and other residues [17] in surface microstructure such as cracks or crevices, or in exposed construction elements such as screws, joints or hinges. It is suggested that all surface corners be radiused and sharp corners be avoided to ease the cleaning [16],[17]. However, the modelling of rounded corners in CAM/CAD application is considered difficult and prone to errors in complex cases [1], and thus alternative modelling strategies are suggested. Skeletal implicit surface modelling allows for generating a smooth and seamless surface from the collection of simple geometry called *skeleton* [5],[6],[14], as illustrated in Figure 1. The technique enables us to create a complex geometry from a collection of separated simple geometries and avoid sharp corner edges.

In principle, implicit surfaces are the contours of a scalar field in three-dimensional space, which are also called an *iso-surfaces*. In skeletal implicit surface modelling, field function is used to determine the potential value for every point in space from the underlying primitive geometry, usually points, lines or bounded planes, as the skeletons. The field function defines the potential value that exponentially decreases according to the distance from a skeleton [5], [6]. In this way, iso-surfaces are the covering surface for each skeleton which is identified as the center of the object. If the skeletons are close enough to one another as illustrated in Figure 1(a), their field values are summed up, resulting in a blended geometry as illustrated in Figure 1(b). The implicit surface is generated in Grasshopper, using an add-on Cocoon [10] based on the *Meta Balls* field function [7]:

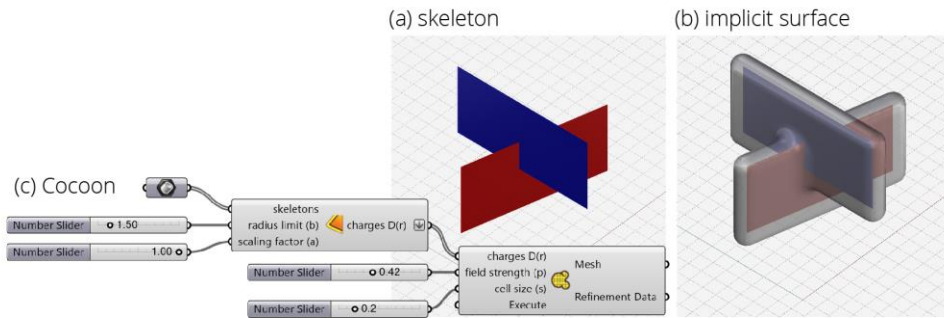


**Figure 1:** Skeletal implicit surface modelling using Cocoon.

$$D_i(r_i) = \begin{cases} a \left(1 - \frac{3r_i^2}{b^2}\right), & 0 \leq r_i \leq b/3 \\ \frac{3a}{2} \left(1 - \frac{r_i}{b}\right)^2, & \frac{b}{3} \leq r_i \leq b \\ 0, & b \leq r_i \end{cases} \quad (2.1)$$

$$p = \sum D_i(r_i) \quad (2.2)$$

The field function  $D_i(r_i)$  determines the field strength within 3D space in which  $r_i$  is the minimum distance of a point in space to the skeleton  $i$ . Radius limit  $b$  defines the maximum distance that bound the effect of the function to a finite value from the skeleton while scaling factor  $a$  multiplies the field strength linearly. The field strength  $p$  in a point in space is defined as the sum of field function  $D_i(r_i)$  of all skeletons as in Equation (2.2). The resulting geometry is identified by determining the value of iso-surface field strength  $p$  in which the surfaces represent all points in space that have field strength  $p$ . Figure 1(c) illustrates the defining parameters involved in skeletal implicit surface modelling implemented in Cocoon. To extract the implicit surface to a workable mesh, a marching cubes algorithm is employed [15]. The cell-size of the marching cubes determines the resolution of the mesh and the number of details that can be captured from the formed iso-surface. The larger the cell-size, the coarser the result. Decreasing the cell-size will result in a smoother and more detailed surface but will also increase the computational cost due to an exponential increase in the number of cells used to detect the surface with the algorithm. Therefore, establishing a balance between the details and the computational cost is key to achieving efficiency in this modelling technique.

For the purpose of this study, the surface shape generated from the skeletal implicit surface modelling will be subjected to the simulation of RJH cleaning. Several parameters of the cleaning process need to be established as the basis for developing the simulation, as discussed below.

## 2.2 Rotary Jet Head Cleaning

The concept of a self-cleaning toilet cubicle using a liquid jet is inspired by the industrial in-tank cleaning technology [25]. It involves projecting a set of jets of cleaning liquid onto surfaces that needs cleaning. The physical impact of the jet provides a cleaning effect on the surface. In industrial cleaning practice, the liquid jet heads rotate in two axes, creating a trajectory pattern that sweeps across the surface [4], [25]. The physical impact of the jet on the point of impingement plays an important role in determining the cleaning effect [25]. Controlling the cleaning pattern is essential to ensure that the jet covers the entire parts of the surface. Normally, the vertical and horizontal motion speeds of the nozzle are set in a slight ratio to create a crossing spiral pattern that can cover the entire surface as illustrated in Figure 2(a).

Computer simulation has been used to determine the optimal positioning of the cleaning device by accounting for flow pattern, volume, and shadow areas affected by the internal structure of the cleaned apparatus [25]. One way to visualise the cleaning distribution is to measure the wetting intensity across the cleaned surface [27]. The visualization in Figure 2(a & b) shows the effect of cleaning pattern and the surface geometry from the impacting jet distribution. Yet, it must be noted that the distribution only shows cleaning liquid distribution density without taking into account the cleaning effect from the geometric and kinematic parameters of jet-surface interaction.

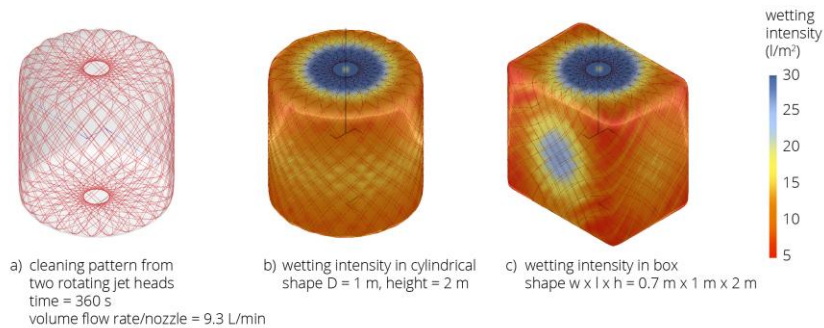


**Figure 2:** Flow pattern and impingement distribution of RJH cleaning.

The use of the analytical model of jet cleaning is favored in cleaning effect prediction due to the high computational cost of CFD simulation [20]. It incorporates the mathematical formulation of impacting liquid jet onto a surface, which is supported by simulation or empirical experiments. Previous studies have addressed different approaches in the physical formulation of liquid jet cleaning phenomenon [4], [10], [21], [28-29]. A removal model is developed to predict the amount of time, liquid, and energy needed in cleaning a soil layer from a surface via peeling mechanism (adhesive failure) [4], extending the previously developed models [28-29]. The model provides a means for predicting the temporal progression of cleaning in several assumed conditions. The specificity of the assumed conditions thereby constraints the model to be applied in more complex cases. This motivated another research to develop an efficient CFD simulation to provide flexibility in predicting the cleaning effect in more complex configuration [19].

While the previous researches aimed at predicting the resources needed to perform cleaning, our aim in this research is to predict the cleanability of a surface configuration that is subjected to RJH cleaning. Thereby, time-based cleaning performance indicator does not fit our purpose which only needs the estimation on how effective one surface can be cleaned in a particular scenario. Compared to the conventional static spraying cleaning that relies on the flushing and rinsing effect, the rotary jet heads cleaning depends more on the mechanical action resulted from the physical impact of the jet impingement [25]. Following the same approach by a study that attempted to predict the cleanability of mechanical component [3], the nozzle parameters, fluid, and target material properties are considered to be fixed. In this way, the cleaning effect can be feasibly calculated from geometry and kinematics description of jet-surface interaction, in which the flow parameters, stand-off distance and impact angle of the jet are assumed to play a significant role in determining cleaning effect. It is also assumed here that the liquid flow rate is high enough to maintain the straight jet trajectories, while the gravity is considered to have a little effect on the cleaning performance.

The cleaning effectiveness of single liquid jet has been found to be correlated with the impact pressure on the impingement point [3][10]. Assuming a circular impact distribution, a study on the influence of jet breakup in industrial-scale provided a model to estimate the mean impact force  $F$  and impact area  $A$  as the functions of jet parameters and the stand-off distance in a horizontal direction as following [10]:

$$F = \frac{4\rho}{\pi} \left( \frac{V}{d_N} \right)^2 (1 - f_1 L f_2)^2; f_1 = 0.013 \text{ m}^{-1}, f_2 = 2.006 \quad (2.3)$$

$$A = \pi \left( L \tan \left( \frac{1}{2} d_1 L^{d_2} \right) \right)^2; d_1 = 2.11 \frac{\text{degree}}{\text{m}}, d_2 = -0.54 \quad (2.4)$$

where  $L$  is the stand-off distance between nozzle and impingement point (m),  $V$  is the volume flow rate of the jet ( $\text{m}^3\text{s}^{-1}$ ),  $d_N$  is the nozzle diameter (m) and  $\rho$  is the liquid density ( $\text{kg}\cdot\text{m}^{-3}$ ). The coefficients  $f_1$ ,  $f_2$ ,  $d_1$  and  $d_2$  are the results of multiple regression for the investigated nozzle ( $d_N=3$  mm and 4 mm) in the study [11]. The impact pressure can  $P$  ( $\text{kg}\cdot\text{m}^{-1}\text{s}^{-2}$ ) be calculated by:

$$P = F/A \quad (2.5)$$

This study implemented the jet parameters as in Fuchs et. al [110]. Following the previous calculations, Figure 3(a) illustrates that the impact pressure drops significantly at a short distance of  $< 0.5$  m then continues to drop at a lower rate at a longer distance. This indicates that the impinging distance below 0.5 m is not a stable range for cleaning.

The impacting liquid jet is not always perpendicular to the surface due to jet heads movement and the shape of the surface. Specifically, an empirical study showed that the impact pressure increases at an inclined impact angle [8]. It was also found that the inclined impact angle could improve cleaning performance due to the increased shear stress in the tilted scenario [2]. The relation between the cleaning effect and the impact angle varies, depending on jet parameters and target material properties. In this case, it is decided that the optimum tilting angle between the jet and the surface is  $15^\circ$  [20]. This flat impact angle can be described by the increase of shear stress, which promotes the thinning and erosion of the soil on the surface [4]. This flat optimum impact angle value is also found in the abrasive water jet cutting for ductile materials [15].

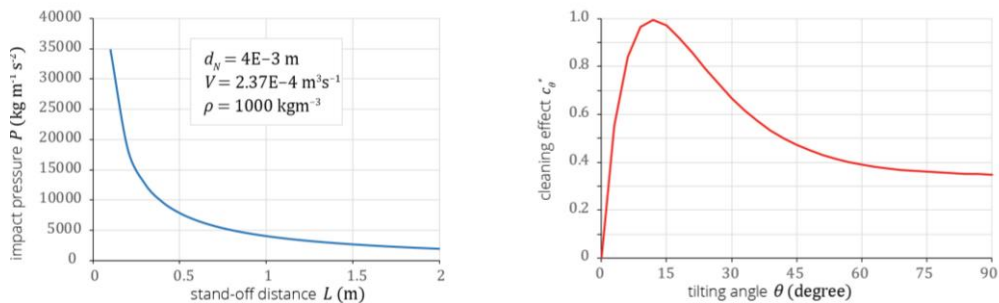


**Figure 3:** Relation between cleaning parameters: (a) The effect of stand-off distance to impact pressure in industrial-scale according to Equation (2.5), (b) The influence of impact angle  $\theta$  to the cleaning effect  $c_\theta^*$ .

Due to the difficulties in finding a model that can explain the relation between impact angle and cleaning effect, we adapted the data from Arbelaez et.al [3] to an equation using curve fitting tool [33]. It compares thousands of templates from a wide range of equation families. We took an equation from its top list and further trim the function to get the following equation:

$$c_\theta^* = -0.6527 (\exp(1.608 - 0.1357 \cdot \theta) - 2 \cdot \exp(0.804 - 6.785 \times 10^{-2} \cdot \theta)); 0^\circ \leq \theta \leq 90^\circ \quad (2.6)$$

where  $c_\theta^*$  represents a dimensionless influence of impact angle  $\theta$  to the cleaning effect as illustrated in Figure 3(b). In this study, it is assumed that the impact pressure and the impact angle are linked

to the cleaning performance. The overall performance of RJH cleaning is tied to the geometrical relation between jet and surface along with the employed cleaning procedure. The shape of the surface and cleaning procedure thus heavily affect this jet-surface interaction. Optimizing the surface geometry in a particular RJH cleaning procedure, therefore, becomes the main focus of this study. The formulation of impact pressure and influence of impact angle to cleaning effect is used in our jet cleaning model for optimization purpose which will be described further.

### 2.3 Parametric Optimization

The purpose of the toilet cubicle surface shape optimization is to achieve a certain level of cleanability in a particular RJH cleaning scenario. There are several optimization algorithms that are already available in Grasshopper. Galapagos is the most popular optimization solver based on Genetic Algorithms (GAs) that mimics the biological evolutionary principles [11]. It works by generating the population of design variants based on the given parameters that are mutating and collating toward the best objective value. The population-based optimization often requires thousands of design evaluations before yielding the best optimal result [31]. On the other hand, the integration of the simulation evaluation into the parametric processes is computationally expensive [32]. Thus, the integration of simulation and evaluation in a parametric optimization approach effectively make the population-based optimizer (i.e. GAs) impractical in its implementation.

To overcome the limitations of GAs, we used Opossum which was developed on model-based optimization principles [28]. This solver works by approximating the simulation result using the surrogate model method which has been proven to exhibit several advantages in architectural optimization by reducing the number of iterations [30]. The accuracy of the surrogate model improves with the number of evaluations completed. Furthermore, there is a number of random simulations that require completion before the solver can accurately predict the optimal design solution. In practice, Opossum needs to complete approximately 15 evaluations before rapid progress is achieved in optimizing the design. Overall, only 200-300 evaluations are required for this solver to yield an optimal solution, which aids time-intensive optimization challenges.

## 3 MODELLING AND OPTIMISATION OF THE SELF-CLEANING PORTABLE TOILET SURFACE

### 3.1 The Objectives

The aim of the development of this modelling and optimization of workflow for cleanability-based design is threefold: first, to demonstrate the potential ability of the skeletal implicit modelling technique as a promising modelling method within the parametric modelling environment; secondly, to develop an adequate rotating liquid jet simulation method to be integrated into parametric modelling; thirdly, to demonstrate the optimization of toilet cubicle design based on cleaning performance. The smooth and deformable properties of the implicit surface provide advantages for cleanability and enable the deformation of the surface without disrupting its continuity. Therefore, these properties enable us to define a parametric model that easily provides a wide range of shapes compared to the standard B-rep modelling method. We used this advantage to model a public toilet cubicle and optimize its shape by measuring cleaning performance through RJH using the optimization solver Opossum.

The modelling and optimization workflow of the portable toilet cubicle consists of these main steps (Fig 4.): (a) skeleton definition, (b) implicit surface generation, (c) mesh selection, (d) rotating liquid jet simulation, (e) objective function definition, and (f) optimization solver. The first three steps of the workflow provide a parameterized, deformable mesh object of the toilet cubicle interior surface using the skeletal implicit surface modelling technique. The rotating liquid jet simulation evaluates the generated mesh object using a particular set of parameters that are relevant to industrial liquid jet cleaning practices. The jet impingement model is developed based on the formulation established in the previous section. The shape of the toilet, as well as the position of

RJH, are subjected to optimization. The interdependency between the surface and the cleaning jets makes the optimal solution lies in the interplay between the surface shape and RJH positions.

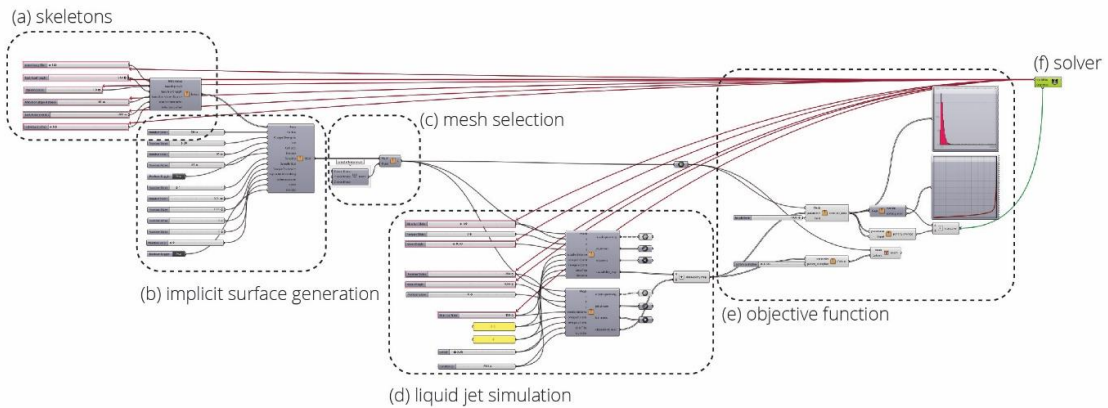


**Figure 4:** Overview of parametric modelling and optimization.

Thus, the main objective of this optimization is to find the best RJH position and surface shape altogether. The objective function of the solver is calculated from the simulation results, in which the solver attempts to maximize and evenly distribute the cleaning on the targeted surface.

### 3.2 Generating Implicit Surface Geometry

Skeletal geometries in Grasshopper allow the parameterization of the resulting surface shape. The incorporation of the skeletal implicit modelling technique allows for the quick generation of smoothed geometry without using a CAD/CAM surface blending algorithm, which does not always guarantee success in cases involving complex shapes. The geometry model was developed based on the common components of public toilet cubicle interior consisting of the cubicle, toilet bowl, and toilet tank, as found in portable toilet design patent documents [23], [27]. We eliminated the smaller details to focus on the shape of the cubicle and toilet to reduce the dimensions of the optimization problem. Figure 5 shows the modelling stages, which include: (a) the formulation of defining parameters (b) the definition of skeleton geometry and its parameters, (c) the definition of implicit modelling boundaries and meshing parameters, (d) the selection of an interior mesh to be evaluated through liquid jet simulation.

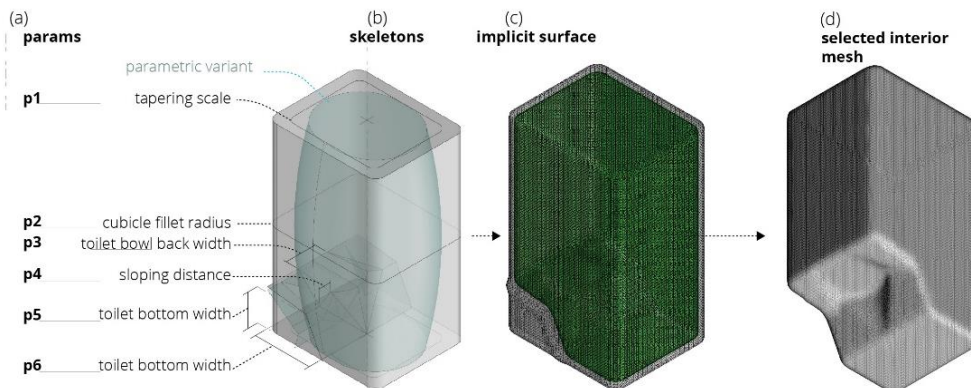


**Figure 5:** Defining the geometry of the toilet cubicle.

The formulation of toilet cubicle shape parameters considers the range of possible shapes pertaining to cleaning without compromising the function of any components of the toilet. We established two parameters  $p_1$  and  $p_2$  for defining the shape of the cubicles and four parameters  $p_3$ ,  $p_4$ ,  $p_5$ , and  $p_6$  for defining the shape of the toilet tank in relation to the toilet bowl. The dimension of the toilet bowl is locked to maintain the usability of the toilet. Based on the defined parameters, two intersecting B-reps were generated as skeletons for creating the implicit surface. We defined the radius limit  $b$ , field strength  $p$  in Cocoon in such a way that the implicit surface is generated at a distance of 25 mm from the skeleton's surface (See Fig 1.). The cell-size of the marching-cubes algorithm in Cocoon is also set at 25 mm to provide sufficient details with a reasonable computing cost. These parameters are the keys in defining the skeletons to obtain a desirable geometry.

### 3.3 Simulation of Rotating Jet Cleaning onto The Surface

To simulate the surface cleaning, we created a set of two rotating liquid jet nozzles that approximate the industrial cleaning pattern by defining its horizontal and vertical axis angular speeds (See Fig. 6.). The two nozzles rotate at defined time step  $\Delta t$ , angular speed vertical  $\omega_v$ , and angular speed horizontal  $\omega_h$ , in a particular position inside the cubicle, generating a series of impingement points across the surface as illustrated in Figure 3.

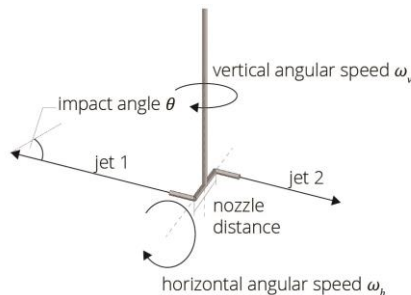


**Figure 6:** Rotating jet impingement model.

For each impingement point, the cleaning effect  $c_p$  ( $\text{kg} \cdot \text{m}^{-1}\text{s}^{-1}$ ) is calculated as the multiplication of time step  $\Delta t$ , impact pressure  $P$  and impact angle influence  $c_\theta$ :

$$c_p = \Delta t \cdot P \cdot c_\theta \quad (3.1)$$

This enables a discrete cleaning effect calculation based on impact pressure and impact angle for all impingement points along with the cleaning pattern. Figure 7(a & b) illustrates how the model creates a series of impingement points for each time step  $\Delta t$  that accumulates over time. The cleaning effect from each impingement point is then mapped into the mesh vertices to be used to calculate cleaning distribution.

For each discrete impingement point  $p$  with cleaning effect  $c_p$ , the value of  $c_p$  is mapped into the three vertices  $v_1, v_2, v_3$  of the triangle mesh face that contained the impingement point according to its areal coordinates (See Fig. 7(c)):

$$p = \lambda_1 v_1 + \lambda_2 v_2 + \lambda_3 v_3 \quad (3.2)$$

where the three positive numbers  $\lambda_1, \lambda_2, \lambda_3$  are the areal coordinates of point  $p$  with respect to the containing mesh triangle [13]. The mapping of the cleaning effect  $c_p$  to the three vertices accordingly:



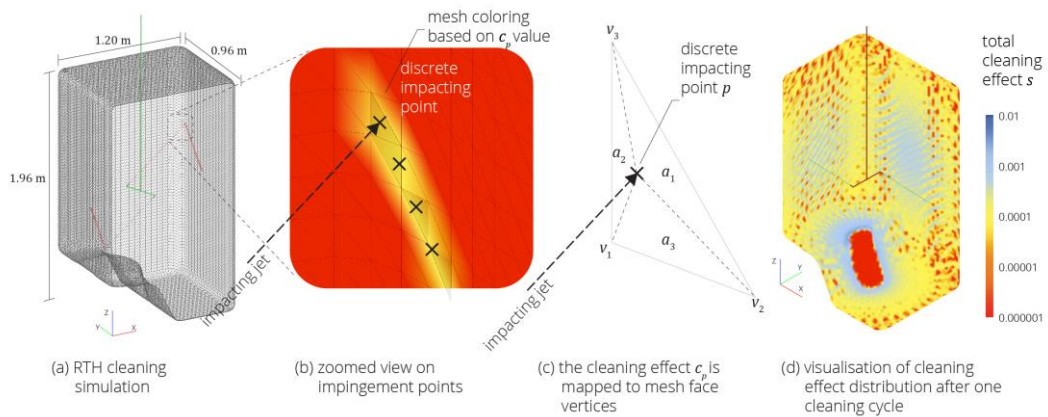


**Figure 7:** The mapping of an impacting jet on a cleaned surface.

$$\begin{aligned}
 c_{p1} &= \lambda_1 \cdot c_p, \\
 c_{p2} &= \lambda_2 \cdot c_p, \\
 c_{p3} &= \lambda_3 \cdot c_p
 \end{aligned}
 \tag{3.3}$$

The mapped cleaning effect within each mesh vertex is summed up as a total cleaning effect per-vertex  $s$ . The total cleaning value of vertices is used to create a cleaning distribution map for the entire surface. The mapping allows the calculation of cleaning performance for the entire surface for optimization purpose. It also enables an easy mesh coloring in Grasshopper to provide a quick qualitative evaluation, as illustrated in Figure 7(d). This is an efficient method to be implemented in Grasshopper, yet it neglects the details such as the impact pressure distribution within the jet impingement area and the cleaning width. It is also assumed that the area mesh faces are similar to one another, which is the case in the meshes generated by the marching cubes algorithm.

A more detailed study is needed to provide a more accurate yet efficient cleaning mapping for optimization purposes. We acknowledged that this model is far from perfect in depicting the complex phenomenon of jet cleaning. However, our focus here is to develop a parametric optimization framework in Grasshopper in which a simple model for predicting the cleanability of a surface geometry from RJH cleaning is used to test the framework. Further studies are needed to provide a better description of jet-surface interaction to be implemented in parametric modelling approach.

### 3.4 Optimization of Surface Cleaning Performance

Our objective is to find the shape of the portable toilet cubicle interior and nozzle position with the optimal levels and coverage of cleaning. The shape of the cubicle, toilet tank, and toilet bowl can be modified by adjusting the six defined parameters, as illustrated in Figure 5. The RJH position can be adjusted by defining its coordinates on the median plane of the cubicle within the defined region area (See Fig. 8). In doing so, the optimal RJH position needs to be established within the defined plane to yield the optimal cleaning result. Another parameter that we adjusted is the distance between the two rotating liquid jet nozzles. This parameter enables various design shapes and nozzle options to be tested simultaneously. It is assumed that the lower part of the surface is the most frequently used part of the cubicle and therefore requires more cleaning effort. The surface part that is within 1 meter above the cubicle ground is defined as the *cleaning priority area*. The optimization focuses on maximizing the cleaning effect on this prioritized surface. Hence, the calculation of the cleaning effect in this optimization is only limited to this area.

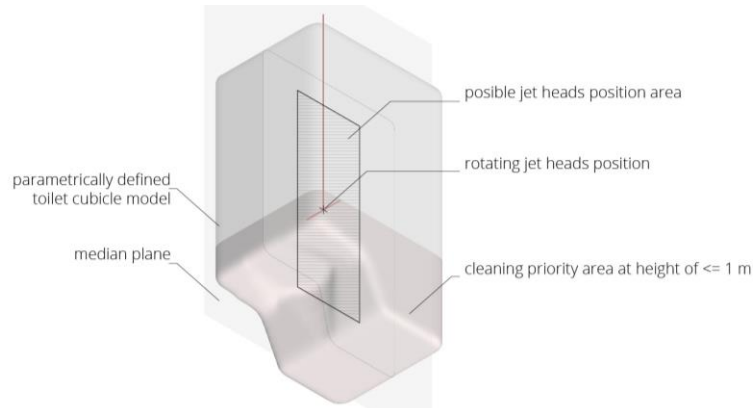


**Figure 8:** The optimization scheme.

Case	Number of Positions	Vertical angular speed (rpm)	Horizontal angular speed (rpm)	Duration for each position (s)	Total cleaning time (s)
case 1	1	3.9	4.0	1200	1200
case 2	2	3.9	4.0	600	1200
case 3	3	3.9	4.05	400	1200

**Table 1:** Three cleaning scenarios for case 1, case 2 and case 3.

This optimization study uses three cleaning scenarios with variation in the RJH positions for the same amount of cleaning time as detailed in Table 1. Case 1 has only one possible RJH stationary position within the defined area in a defined period of time. In case 2, the RJH has two possible stationary positions, with the duration of cleaning for each position half of the duration in case 1. Case 3 employs three possible RJH stationary positions within the same amount of time. The purpose of optimization is to find the best position for RJH in each case, along with the shape of the toilet. These three cases were selected to see the effect of RJH positions on the shape of the toilet.

Cleanability was tested by assuming a set of two rotating liquid jet nozzles within the relevant parameters for industrial conditions found in Fuchs et. al [10]. We used two heads of the 4 mm jet nozzle at a pressure of 0.3 MPa, which resulted in  $1.7 \text{ m}^3\text{h}^{-1}$  liquid consumption. In the industrial cleaning practice using RJH, the number of heads ranges between two and eight, with normal flow rate ranges from  $2\text{-}30 \text{ m}^3\text{h}^{-1}$  at a pressure range of 0.3-0.8 MPa [26]. The jetting parameters used in this study are near the lower range of the industrial standards, which can be explained by the relatively small cleaning size.

An initial test was performed to find the optimum time step by conducting RJH simulation with the time steps of 0.2, 0.1, 0.05, 0.25 and 0.125 seconds. The comparison of the cleaning effect values from each simulation indicates that the median of cleaning effect collected from all vertices increases along with the decrease of the time step and is converged at the time step of 0.05 seconds. The peak value of the cleaning effect was decreasing and converged at the same time step. Base on this initial test, the time step of 0.05 is used for the optimization study.

The objective function is formulated in terms of the cleaning effect collected from all vertices of the prioritized surface, in order to identify the optimum configuration of the surface and RJH position with the maximum distribution of cleaning effect for the entire prioritized surface. Let  $s$  be the total cleaning effect of each vertex of the mesh in the prioritized surface,  $med(s)$  be the median of all  $s$  from the mesh vertices, and  $p_i(s)$  be the penalty value if the value  $s_i$  is lower than half of the median  $med(s)$ , where  $i$  be the index of vertex. The expression  $p_i(s)$  aims to enable a penalty for surface areas that exhibit low cleaning effect, thus promoting a more balanced cleaning distribution. The

use of a median is preferred due to the existence of extreme values related to the cleaning effect for which an average does not provide a strong reading of distribution centrality. The maximization objective is defined as the median of the total cleaning effect for each vertex  $med(s)$  added to the average of penalties for every vertices  $p_i(s)$  where  $n$  is the number of vertices:

$$\max f(s) = med(s) + \frac{1}{n} \sum_{i=0}^n p_i(s) \quad (3.1)$$

$$p_i(s) = \begin{cases} 0, & s_i \geq \frac{1}{2} \cdot med(s) \\ -med(s) \cdot \cos\left(\frac{s_i}{med(s)}\pi\right), & s_i < \frac{1}{2} \cdot med(s) \end{cases} \quad (3.2)$$

Due to the cubicle shape and the variation in RJH positions, the two nozzles are sometimes located outside the cubicle wall and resulted in an error in cleaning effect calculation. In this case, the value of  $f(s)$  is set to zero. This condition is suboptimal because it increases the number of unnecessary iteration. Further development is needed to provide a better error handling method. In evaluating the objective, the jet impingement simulation generated 48,000 jet impact points on approximately 30,000 mesh faces. In addition to implicit surface geometry generation, it takes approximately 35 seconds for each evaluation to be conducted using Intel Core i7 6500U 2.50GHz CPU. We set the Opossum optimization solver to have 300 iterations using the default optimization settings. The whole process took around 3 hours to complete.

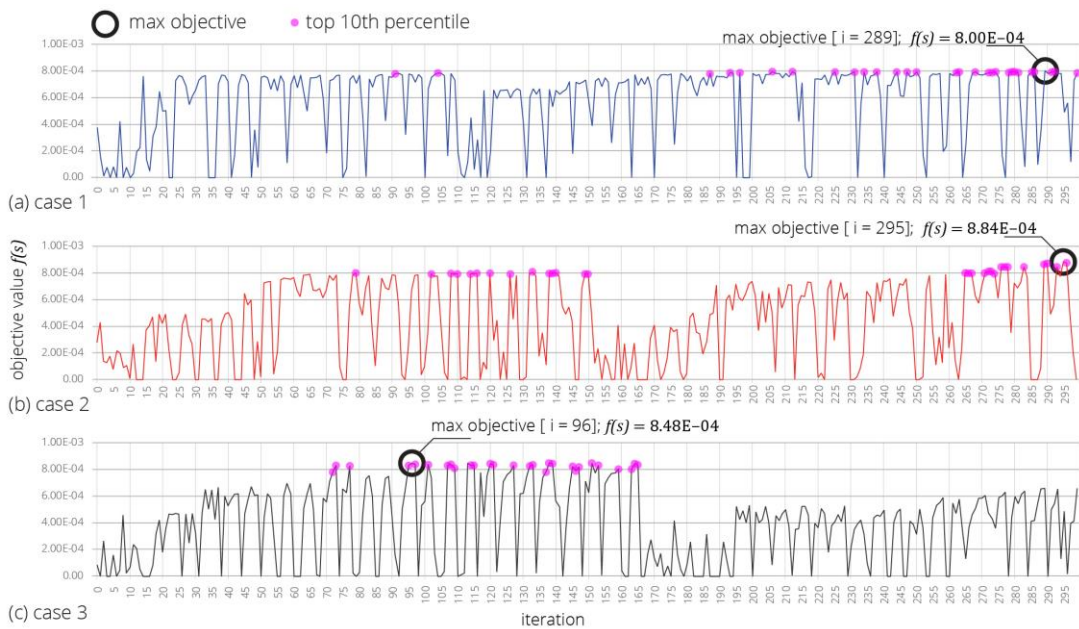
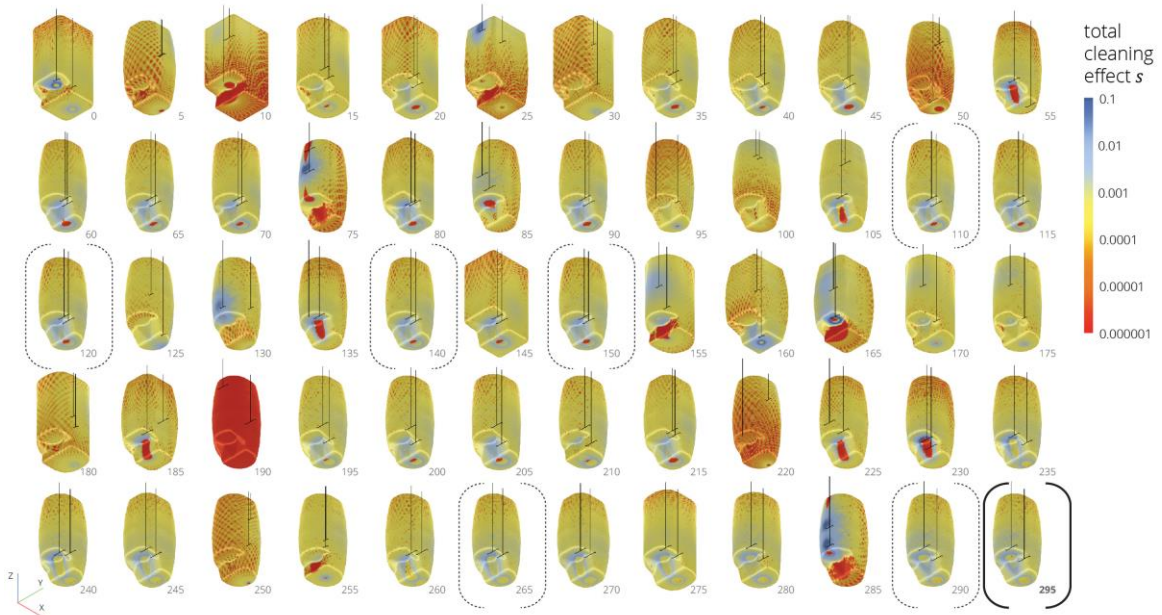


**Figure 9:** The progression of objective value during iteration, the final result is highlighted.

#### 4 RESULTS AND DISCUSSION

Figure 9 shows the progression of the objective value during 300 iterations in the three cases. The result of the optimization is highlighted by a black circle and the top 10<sup>th</sup> percentile of iteration is highlighted by cyan circles. The zero values of objective value  $f(s)$  persist if the RJH lies outside the cubicle. It is shown that the solver found near-optimal results in the early half of iterations. However, the solver starts over the search in the later stage of optimization without further increasing its

objective value, then terminated after reaching the iteration limit. The solver found the high objective value in the earlier iteration of case 01 (a) as compared to case 02 (b) and case 03 (c). It is likely that the additional number of RJH position increases the dimension of the search space of the optimization problem, thus prolonging the search. It is also noted that the optimal value is not always found in the final iterations as in case 3 where the maximum objective value was found at the 96<sup>th</sup> iteration.



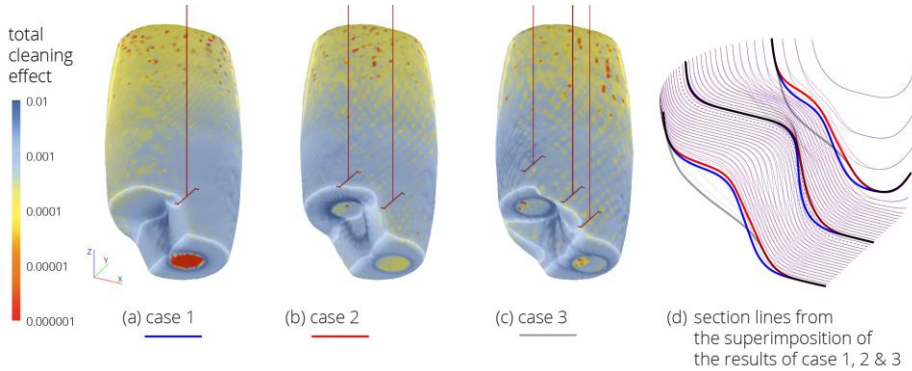
**Figure 10:** The visualization of case 2 optimization iterations, the final result and the top percentile are highlighted.

Figure 10 illustrates the evolution of cubicle shape during the iteration in case 2 optimization, with an interval of five iterations. The final optimization result is highlighted with solid lines and the top 10<sup>th</sup> percentile is highlighted with the dashed lines. The shape and the position of RJH change simultaneously during optimization until the final iteration is reached. The closer look at the top percentile of the solutions suggests that the cubicle shapes are similar with slightly different RJH positions.

The results provide an insight into how the optimum cleanability performance of the portable toilet interior surface can be achieved by adjusting the shape of the surface and RJH positions. The optimization result of the three cases are illustrated in Figure 11(a, b & c) while Figure 11(d) shows the superimposition that highlight the differences among the cases. All the three cases suggested a heavily tapered and rounded cubicle, which generally provides a more balanced cleaning distribution and minimizes the impingement distance from the far corner. The toilet tank shape was also optimized as such to minimize the narrow corners.

There were slight differences in the slope of the toilet water tank among the cases except case 3. In case 1, the RJH was positioned to avoid shadowing with the tank shape. The tank slope is also steeper, as shown in Figure 11(d) in blue lines, possibly to provide a shallower impact angle from RJH to maximize the cleaning effect. The distance between the two opposite nozzles was lengthened into its maximum possible value (30 cm), resulting in a small amount of circle area unreachable by the rotating jets. Further analysis indicated that minimizing the distance between the rotating nozzles could decrease the penalty value since it reduced the uncleaned circle area. However, it was overcome by the fact that the general cleaning effect was reduced significantly due to the decreasing stand-off distance between the nozzle and the surface, which resulted in a lower objective value.

This is particularly true for the small-size toilet cubicle in which even a small alteration of the distance creates a significant effect on the impact pressure (Fig 4.).



**Figure 11:** The optimization results of case 1, case 2 and case 3.

In case 2 (b), the RJH was set at the positions that avoid shadowing with the tank. The slopes of the toilet tank, represented in red lines in Figure 11(d), were slightly shallower compared to the case 1 (a), perhaps to minimize the distance to the closest RJH. Different tank shape was resulted in case 3 (c) as represented in grey lines in Figure 11(d). The tank shape has shallower slopes compared to the other cases, which resulted in fairly more complex geometry. The number of multiple RJH position allows a more complex shape to be effectively cleaned. The multiple positions also result in a better cleaning distribution as indicated by the fewer amount of under cleaned surface area.

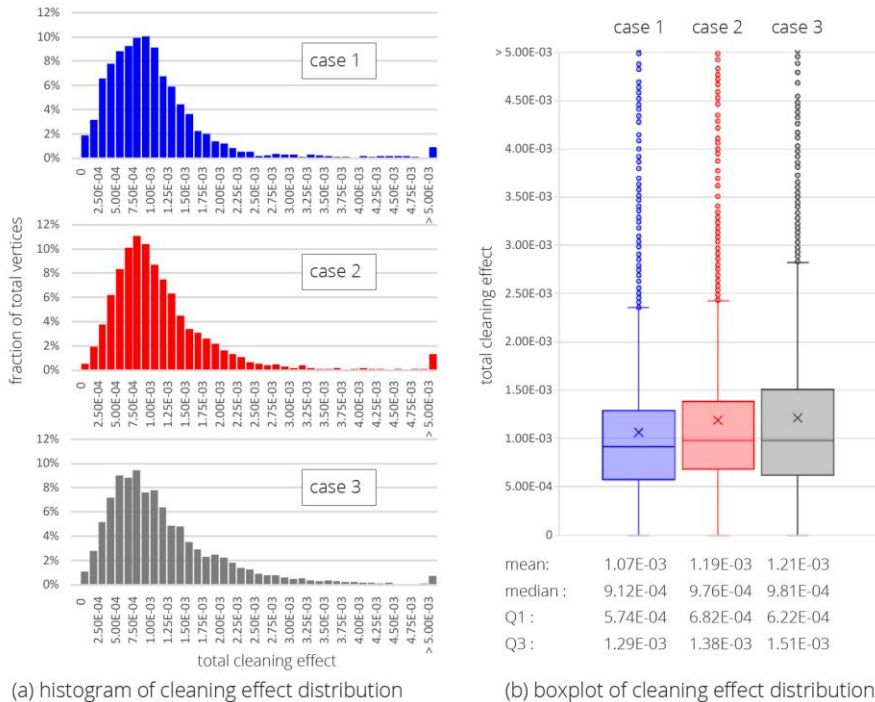


**Figure 12:** The comparison of the distribution of the cleaning effect.

The histogram in Figure 12(a) illustrates the cleaning distribution of the three cases in the fraction of total vertices. Case 1 distribution is slightly skewed to the right, indicating many areas that are potentially under cleaned as also indicated by the lower mean and median in boxplot in Figure 12(b). This distribution is likely due to the use of a single stationary RJH position. Case 2 has a good cleaning distribution with a smaller fraction of area that has low cleaning effect compared to the other two cases. The box plot shows a narrow interquartile range, indicating a relatively balanced cleaning distribution. Interestingly the distribution of cleaning effect in case 3 is wider than the other cases, with the highest mean and median value. It suggests that there are areas potentially over and under cleaned in this case. This shows that the median statistical figure alone is not sufficient to fully describe the optimal solution. Thus, it is necessary to incorporate a more complete statistical figure in objective values to improve the optimization.

These three cases show that the distribution of RJH cleaning effect for a set of configured surfaces can be described as a function of surface shape and RJH parameters that include position and motion. The three cases show similarities in terms of shape optimization, which tends to minimize the narrow corners and to shorten the distance from the impinging jet nozzle. It is possible that these resulting similarities are also due to the particularly small size of the cubicle, and, therefore, the number of possible surface configurations is fairly limited. We also found that our objective function can be improved to provide better feedback to the solver in the optimization process.

## 5 CONCLUSIONS

This study demonstrated the possibility of surface cleaning performance improvement by employing the optimization of parametrically defined skeletal implicit model surfaces that are subjected to the liquid jet cleaning technique. The use of skeletal implicit modelling technique in hygiene-oriented surface optimization is particularly relevant due to its ability to produce a smooth parametric deformable surface which provides a wide range of surface configuration variants to be evaluated. The distribution of cleaning effect using the RJH for a set of configured surfaces is found to be the function of surface shape and jetting parameters, which include the position and the motion of the liquid jet nozzles. Due to high computational costs for the modelling and simulation technique with higher levels of detail, in this study, we used a general level of detail to provide a basic cleanable shape of the toilet cubicle surface. Further investigation is needed to perform a more detailed design optimization that can address the different levels of detail.

A simple model of liquid jet impingement is used for evaluating surface cleaning performance in particular liquid jet cleaning conditions. The availability of a model of liquid jet impingement allows the calculation to be scripted and implemented into the parametric modelling environment, such as Grasshopper. Further studies are necessary to improve and validate the model. A more accurate jet cleaning model thereby will open the possibility of including more cleaning efficiency variables such as liquid consumption, time and other cleaning resources. Future research suggests the need for multidisciplinary efforts combined with engineering and architectural design to provide an efficient design approach to improve the hygienic performance of public facilities.

## ACKNOWLEDGMENT

This research is supported by the United States Agency for International Development (USAID) through the Sustainable Higher Education Research Alliance (SHERA) Program for Universitas Indonesia's Scientific Modeling, Application, Research and Training for City-Centered Innovation and Technology (SMART CITY) Project, Grant #AID-497-A-1600004, Sub Grant #IIE-00000078-UI-1.

Mikhael Johanes, <http://orcid.org/0000-0002-4097-0517>  
 Paramita Atmodiwirjo, <http://orcid.org/0000-0002-7182-5531>  
 Yandi Andri Yatmo, <http://orcid.org/0000-0001-5393-231X>

## REFERENCES

- [1] Alhashim, I.: Blending operations using rolling-ball filleting, 2009, [https://ialhashim.github.io/files/documents/rollingball\\_fillet\\_report.pdf](https://ialhashim.github.io/files/documents/rollingball_fillet_report.pdf)
- [2] Anglani, F.; Barry, J.; Dekkers, W.: A numerical study on high-pressure water-spray cleaning for CSP reflectors, AIP Conference Proceedings, 1734, 2016, 160001. <https://doi.org/10.1063/1.4949242>
- [3] Arbelaez, D.; Avila, M. C.; Krishnamurthy, A.; Li, W.; Yasui, Y.; Dornfied, D.; McMains, S.: Cleanability of mechanical components, Proceedings of 2008 NSF Engineering Research and Innovation Conference, 2008, <https://escholarship.org/uc/item/5d53v8cw> .
- [4] Bhagat, R. K.; Perera, A. M.; Wilson, D. I.: Cleaning vessel walls by moving water jets: simple models and supporting experiments, Food and Bioproducts Processing, 102, 2017, 31–54. <https://doi.org/10.1016/j.fbp.2016.11.011>
- [5] Bloomenthal, J.; Shoemake, K.: Convolution surfaces, ACM SIGGRAPH Computer Graphics, 25(4), 1991, 251-256. <http://doi.acm.org/10.1145/122719.122757>
- [6] Bourke, P.: Implicit surfaces, 1997, <http://paulbourke.net/geometry/impliciturf/>.
- [7] Brand, S.: How Buildings Learn: What Happens After They're Built, Penguin Books, London, 1995.
- [8] Brown, K. J.; Kalata, W.; Schick, R. J.; Sami, M.; Maruszewski, A.; Parihar, A.: Experimental and computational study of a spray at multiple injection angles impact study of a clean in place tank wash system, ILASS-Americas 2010 Conference Papers, ILASS-Americas, 2010, <http://www.ilass.org/2/conferencepapers/ILASS2010-181.pdf>.
- [9] Cocoon, <http://www.bespokegeometry.com/2015/07/22/cocoon/>, David Stasiuk.
- [10] Fuchs, E.; Köhler, H.; Majschak, J.-P.: Measurement of the impact force and pressure of water jets under the influence of jet break-up, Chemie Ingenieur Technik, 91(4), 2019, 455-466.
- [11] Galapagos, <https://www.grasshopper3d.com/group/galapagos>, David Rutten.
- [12] Gerber, D. J.; Lin, S.-H. E.; Designing in complexity: Simulation, integration, and multidisciplinary design optimization for architecture, SIMULATION, 90(8), 2014, 936–959. <https://doi.org/10.1177/0037549713482027>
- [13] Gold, C.: Spatial context: an introduction to fundamental computer algorithms for spatial analysis, CRC Press, London, 2016.
- [14] Gomes, A. J. P.; Voiculescu, I.; Jorge, J.; Wyvill, B.; Galbraith, C.: Implicit curves and surfaces: mathematics, data structures and algorithms, 1st ed, Springer-Verlag, London, 2009.
- [15] Hashish, M.: The effect of beam angle in abrasive-waterjet machining, Journal of Engineering for Industry, 115(1), 1993, 51-56. <https://doi.org/10.1115/1.2901638>
- [16] Hasting, A. P. M.: Designing for cleanability, Cleaning-in-Place: Dairy, Food and Beverage Operations, 2008, 81–107. <https://doi.org/10.1002/9781444302240.ch5>
- [17] Hofmann, J.; Åkesson, S.; Curiel, G.; Wouters, P.; Timperley, A.: Hygienic Design Principles, EHEDG Guidelines, European Hygienic Engineering & Design Group, Frankfurt, 2018, <https://www.ehedg.org/guidelines/>.
- [18] Johanes, M.; Atmodiwirjo, P.; Yatmo, Y.A.: Developing digital design workflow for architecture based on cleanability as a design parameter, IOP Conference Series: Earth and Environmental Science, 195, 2018, 012091. <https://doi.org/10.1088/1755-1315/195/1/012091>
- [19] Joppa, M.; Köhler, H.; Kricke, S.; Majschak, J.-P.; Fröhlich, J.; Rüdiger, F.: Simulation of jet cleaning: diffusion model for swellable soils, Food and Bioproducts Processing, 113, 2019, 168-176. <https://doi.org/10.1016/j.fbp.2018.11.007>
- [20] Krishnamurthy, A.; Li, W.; McMains, S.: Simulation and optimization of the water-jet cleaning process, ASME 2009 International Design Engineering Technical Conferences and Computers and Information in Engineering, 5, 2009. 891-898. <https://doi.org/10.1115/DETC2009-86882>
- [21] Leu, M.C.; Meng, P.; Geskin, E.S.; Tismeneskiy, L.: Mathematical modeling and experimental verification of stationary waterjet cleaning process. Journal of Manufacturing Science and Engineering, 120(3), 1998, 571- 579. <https://doi.org/10.1115/1.2830161>
- [22] Lupton, E.; Miller, J. A.: Bathroom, the Kitchen, and the Aesthetics of Waste, Princeton Architectural Press, New York, 1996.

- [23] Mullett, R. M.; Kostelyk, J.; Tyler, D.G.: Knockdown portable toilet, PatentUS6427256B1, USA, 2002, <https://patents.google.com/patent/US6427256B1/en>.
- [24] Oxman, R.: Performance-based design: current practices and research issues. *International Journal of Architectural Computing*, 6(1), 2008; 6: 1–17. <https://doi.org/10.1260/147807708784640090>
- [25] Packman, R.; Knudsen, B.; Hansen, I.: Perspectives in tank cleaning: hygiene requirements, device selection, risk evaluation and management responsibility, *Cleaning-in-Place: Dairy, Food and Beverage Operations*, 2008, 108–145. <https://doi.org/10.1002/9781444302240.ch6>
- [26] Tamime, A.Y.: *Cleaning-in-place: Dairy, Food and Beverage Operations*, 3rd edition, Blackwell Publishing, Oxford, 2008.
- [27] Walraven, H.: Portable sanitation unit, Patent US6370706B1, USA, 1999, <https://patents.google.com/patent/US6370706B1/en>.
- [28] Wilson, D. I.; Atkinson, P; Köhler, H.; Mauermann, M.; Stoye, H.; et al.: Cleaning of soft-solid soil layers on vertical and horizontal surfaces by stationary coherent impinging liquid jets, *Chemical Engineering Science*, 109, 2014, 183–196. <https://doi.org/10.1016/j.ces.2014.01.034>
- [29] Wilson, D.I.; Köhler, H.; Cai, L.; Majschak, J.-P.; Davidson, J. F.: Cleaning of a model food soil from horizontal plates by a moving vertical water jet, *Chemical Engineering Science*, 123, 2015, 450–459. <https://doi.org/10.1016/j.ces.2014.11.006>
- [30] Wortmann, T.; Costa, A.; Nannicini, G.; Schroepfer, T.: Advantages of surrogate models for architectural design optimization, *Artificial Intelligence for Engineering Design, Analysis and Manufacturing*, 29(4), 2015, 471–481. <https://doi.org/10.1017/S0890060415000451>
- [31] Wortmann, T.; Nannicini, G.: Introduction to architectural design optimization, *City Networks: Collaboration and Planning for Health and Sustainability*, Springer International Publishing, 2007, 259–278. [https://doi.org/10.1007/978-3-319-65338-9\\_14](https://doi.org/10.1007/978-3-319-65338-9_14)
- [32] Wortmann, T.: Model-based optimization for architectural design: optimizing daylight and glare in Grasshopper, *Technology|Architecture + Design*, 1(2), 2017, 176–185. <https://doi.org/10.1080/24751448.2017.1354615#>
- [33] ZunZunSite3, <http://zunzun.com/>, James Phillips.